

# Noise enhancement of pattern discrimination in temporal coding

Juliana Martins de Assis and Francisco M. de Assis

**Abstract**—Temporal coding is one mechanism of neuronal information processing. In this paper, we investigated whether there is a significant contribution of extrinsic noise in temporal coding, quantitatively. In order to do so, we simulated different patterns through white noise current, and we used the celebrated Hodgkin-Huxley model to obtain interspike intervals. Then, we fitted gamma distribution to the interspike interval histograms of each pattern and we estimated parameters of shape and rate in each case. These estimated parameters enabled the calculation of information measures, such as differential entropy. These information measures provided us evidence of the improved extrinsic noise contribution to the discrimination of patterns in neuronal temporal coding, when compared to the contribution of mean value of synaptic current.

**Keywords**—Temporal coding, Entropy, Interspike Interval, Hodgkin-Huxley.

## I. INTRODUCTION

In computer science, patterns are related to regularities in data that computer algorithms may find. These regularities may be used in data classification, for example [4]. Similarly, in the nervous tissue, neurons receive patterns. But these patterns are related to the joint activity of many other neurons, or to the environmental stimuli, whether neurons are in the central or peripheral nervous systems.

We can think about the nervous system as a pattern recognition machine. All animals need to interpret the environment in order to survive. According to neuroscience, most of information in nervous system is processed in neurons [2]. Neuronal sensing, processing and coding information enabled animal survival and evolution. Also, neurons collectively have enabled the development of higher and complex cognitive functions.

In the context of sensory data, for example, there are different mechanisms by which neurons process information. For example, latency coding is the mechanism where first spike timing relative from stimulus presentation encodes the stimulus to which neuron is submitted [27]. Other encoding mechanisms include rate and temporal codings [9]. The latter stands for the mechanism where interspike interval (ISI) encodes information from the presented stimulus.

As many other neuronal features, ISI observed in neurons is random. The randomness in interspike interval is due to intrinsic and extrinsic noise. Intrinsic noise is associated to the

random open and closing of ion channels, whereas extrinsic noise is associated to random synaptic input [6].

Typically, in engineering systems, noise constitutes a factor that impairs information transmission. However, noise may improve information transmission in nonlinear systems. A notorious example is the phenomenon of stochastic resonance [3]. In this phenomenon, the transmission of a periodic signal in nonlinear systems is augmented through the addition of noise in a certain level. Different research groups have reported stochastic resonance in several neural systems (see [7] and references therein). Another mechanism where noise improves a signal is called coherence resonance [19], which has implications in visual sensory information processing [20]. Recently, [14] demonstrated signal transmission enhancement through presynaptic noise, in the context of latency coding, using a stochastic perfect integrate-and-fire neuronal model.

In cortical neurons, there is one essential input, which is a synaptic current that presents a mean and a standard deviation. Some questions of interest here are: how the ISI distribution is sensible to each parameter, mean and standard deviation? Additionally, how does the ISI differential entropy change in response to these parameters variations? This last question is an interesting one, in the context of temporal coding, since differential entropy is an information measure, with implications to information coding. In this paper, we aim to answer the aforementioned questions using the Hodgkin-Huxley model, one of the most successful quantitative computational models in neuroscience [8], [12].

The rest of the paper is organized as follows. Section II explains the methodology used in this paper. Section III reveals and discusses the results and Section IV concludes the paper. In the remaining of the text, the operators  $E(\cdot)$  and  $V(\cdot)$  denote expected value and variance, respectively.

## II. MATERIALS AND METHODS

### A. Simulation

In order to understand the capability of neurons to discriminate different patterns, the first step was to model which were the different patterns to which neurons are submitted. Reference [16] reported that, specially in the cortex, neurons are excited by a synaptic current which resembles white Gaussian noise. Moreover, reference [25] models this current as:

$$I(t) = \mu + \sigma \frac{dW}{dt}, \quad (1)$$

where  $\mu$  is a drift and  $\sigma$  is diffusion parameter.  $W$  is a standard Wiener process, thus, it is a process with independent increments, and  $dW$  is the realization of a normal random

variable with zero mean and variance equal to the  $dt$ . The time derivative of Wiener process is a white Gaussian noise [18]. If we approximate  $\frac{dW}{dt}$  as  $\frac{\Delta W}{\Delta t}$ , where  $\Delta W \sim \mathcal{N}(0, \Delta t)$ , we have for each time instant:

$$\begin{aligned} I_k &= \mu + \sigma \frac{\Delta W}{\Delta t}, \\ E(I_k) &= \mu, \\ V(I_k) &= \frac{\sigma^2}{\Delta t^2} V(\Delta W) = \frac{\sigma^2}{\Delta t^2} \Delta t = \frac{\sigma^2}{\Delta t}. \end{aligned} \quad (2)$$

Thus, the drift parameter is the mean synaptic current at each time instant, and the diffusion parameter is related to the current variance at each time instant.

The Hodgkin-Huxley model presents the following equations [10]:

$$\begin{aligned} C \frac{dU}{dt} &= I - \bar{g}_K n^4 (U - E_K) - \bar{g}_{Na} m^3 h (U - E_{Na}) \\ &\quad - g_L (U - E_L) \\ \frac{dn}{dt} &= \alpha_n(U)(1 - n) - \beta_n(U)n \\ \frac{dm}{dt} &= \alpha_m(U)(1 - m) - \beta_m(U)m \\ \frac{dh}{dt} &= \alpha_h(U)(1 - h) - \beta_h(U)h. \end{aligned} \quad (3)$$

In the paper,  $I$  is the synaptic current given as in equation (1). In this nonlinear system of differential equations,  $U$  is the membrane potential,  $C = 1 \mu\text{F}/\text{cm}^2$  is the capacitance of the neuronal membrane,  $\bar{g}_K = 36 \text{ mS}/\text{cm}^2$  is the maximal conductance of potassium channels,  $\bar{g}_{Na} = 120 \text{ mS}/\text{cm}^2$  is the maximal conductance of sodium channels,  $g_L = 0.3 \text{ mS}/\text{cm}^2$  is the conductance of the leakage current (capacitance, current and conductance are normalized by area units). The state variables  $n$ ,  $m$  and  $h$  are activation/inactivation gate variables, and  $\alpha_m$ ,  $\alpha_n$ ,  $\alpha_h$ ,  $\beta_m$ ,  $\beta_n$  and  $\beta_h$  are functions of the membrane potential  $U$ :

$$\begin{aligned} \alpha_n(U) &= \frac{0.01(10 - U)}{\exp\left(\frac{10 - U}{10}\right) - 1} \\ \beta_n(U) &= 0.125 \exp\left(\frac{-U}{80}\right) \\ \alpha_m(U) &= \frac{0.1(25 - U)}{\exp\left(\frac{25 - U}{10}\right) - 1} \\ \beta_m(U) &= 4 \exp\left(\frac{-U}{18}\right) \\ \alpha_h(U) &= 0.07 \exp\left(\frac{-U}{20}\right) \\ \beta_h(U) &= \frac{1}{\exp\left(\frac{30 - U}{10}\right) + 1} \end{aligned} \quad (4)$$

These equations are used with a shifted membrane potential of 65 mV, so the resting potential of the membrane is  $U \approx 0$ .

The shifted values for  $E_K$ ,  $E_{Na}$  and  $E_L$  are -12 mV, 120 mV and 10.6 mV, respectively.

We set  $\Delta t = 0.01$  ms in Euler method as a numerical approximation to obtain the state variable  $U$ , in order to achieve spike times and ISIs. We calculated spike times when the membrane potential was increasing and reached 35 mV, as in [17]. Moreover, we also filtered membrane potential through a moving average filter, which took 200 values to perform filtering. We wrote the simulation code in Python.

### B. Information measures

In order to address how neurons discriminate different patterns, as mentioned in Section I, we used an information measure, differential entropy, which is, in the context of continuous random variables, related to the volume of the set with most of probability [5], and is mathematically defined as:

$$h(f) = - \int_S f(x) \ln f(x) dx, \quad (5)$$

where  $S$  stands for the support of the random variable  $X$  with probability density function  $f(x)$ . We chose to use differential entropy as it is related to the uncertainty of the continuous random variable ISI, which has implications in how one could code its information.

## III. RESULTS AND DISCUSSION

Firstly, with the methods described in Section II, we simulated different patterns represented by different parameter pairs of synaptic current:  $(\mu, \sigma)$ . Specifically, we tested the values for  $\mu$ : 0, 0.2 and 0.4  $\mu\text{A}/\text{cm}^2$ . For  $\sigma$ , we tested the values 1.5, 1.7 and 1.9  $\mu\text{A}/\text{cm}^2$ . In our simulations we observed the first 300 interspike intervals, registering the rate (in spikes per second) and the local variation of ISIs, to examine whether the simulated parameter pairs were biologically feasible. Local variation is a measure of spike pattern irregularity [22] and is given by  $1/(n-1) \cdot \sum_{i=1}^{n-1} (3(X_i - X_{i+1})^2 / (X_i + X_{i+1})^2)$ , where  $X_i$  is the  $i$ -th ISI registered. Table I presents these first results. We observe that the obtained values for these statistics are consistent with those reported in other papers. For example, reference [21] mentions rates from less than 1 spike per second to several tens of spikes per second. Moreover, reference [22] mentions around 0.78 as one typical value for local variation in the cortex of awake behaving monkeys.

TABLE I  
RATE AND LOCAL VARIATION WITH SIMULATED PARAMETERS ( $\mu$  AND  $\sigma$  IN  $\mu\text{A}/\text{CM}^2$ ).

$(\mu, \sigma)$	Rate	Local variation
(0, 1.5)	2.66	0.86
(0, 1.7)	5.40	0.82
(0, 1.9)	9.26	0.61
(0.2, 1.5)	3.07	0.85
(0.2, 1.7)	6.74	0.68
(0.2, 1.9)	10.27	0.64
(0.4, 1.5)	3.61	0.86
(0.4, 1.7)	7.25	0.76
(0.4, 1.9)	10.95	0.57

Secondly, we searched for probability distributions that would have adequate fit for ISI histograms obtained in each pattern (with each parameter pair). For an integrate-and-fire neuronal model, ISIs are independent and identically distributed as inverse Gaussian [14]. However, to the best of our knowledge, there is not a mathematical treatment that determines ISI distribution in a Hodgkin-Huxley model when white noise current is applied. Some references with data from electrophysiological recordings model ISI as gamma, exponential or inverse Gaussian distributed (see references [1], [23], and [15] for example). Exponential is a particular case of gamma distribution, which is a maximum entropy distribution [11]. There is evidence that gamma distribution presents good fit for modeling ISI typically greater than 20 ms [1]. Since most of the ISIs obtained in our simulations are greater than 20 ms, we chose to make an adjustment of ISI histograms with gamma distribution. Gamma distribution has the following density:

$$f_X(x; \eta, \lambda) = \frac{\lambda^\eta}{\Gamma(\eta)} x^{\eta-1} e^{-\lambda x}, \quad x > 0, \quad (6)$$

where  $\lambda > 0$  is a rate parameter and  $\eta > 0$  is the shape parameter. Also, for a gamma distributed ISI  $X$ , we have mean

$$E(X) = \frac{\eta}{\lambda}, \quad (7)$$

and variance

$$V(X) = \frac{\eta}{\lambda^2}. \quad (8)$$

There is not a closed solution for maximum likelihood estimators for parameters  $\eta$  and  $\lambda$  [13]. Using the method of moments, we obtained the estimates:

$$\hat{\eta} = \frac{\bar{X}^2}{S_X^2}, \quad (9)$$

$$\hat{\lambda} = \frac{\bar{X}}{S_X^2}. \quad (10)$$

where  $S_X^2 = \sum_{i=1}^n (X_i - \bar{X})^2 / (n - 1)$ . We used 300 ISIs from each setting to build histograms and 5 bins. Since the distribution of ISIs is usually very asymmetrical and right-skewed, we decided to use nonuniform bins, from 0 to 50 ms, from 50 ms to 100 ms, from 100 ms to 200 ms, from 200 ms to 300 ms and from 300 ms beyond, to all simulated situations. Figures 1, 2, 3, 4, 5, 6, 7, 8 and 9 present us the resulting histograms and fitted gamma densities for all the simulated pairs of synaptic input. Additionally, we performed  $\chi^2$  test for goodness of fit, and we obtained the values indicated in Table II, which also has the values of estimated parameters. The  $p$ -values found in all simulated patterns may not reject our assumption that ISIs are gamma distributed with the estimated values for  $\eta$  and  $\lambda$ , at least at significance levels such as 1% or 5%.

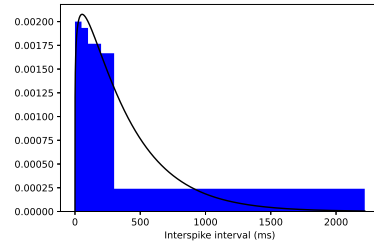


Fig. 1. Resulting ISI histogram and adjusted gamma for parameters:  $\mu = 0$ ,  $\sigma = 1.5$ .

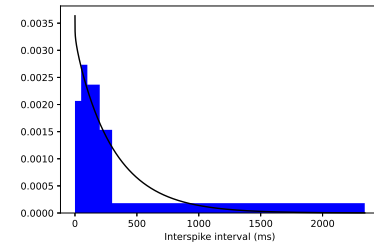


Fig. 2. Resulting ISI histogram and adjusted gamma for parameters:  $\mu = 0.2$ ,  $\sigma = 1.5$ .

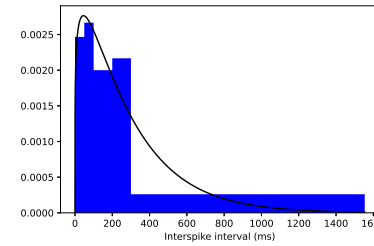


Fig. 3. Resulting ISI histogram and adjusted gamma for parameters:  $\mu = 0.4$ ,  $\sigma = 1.5$ .

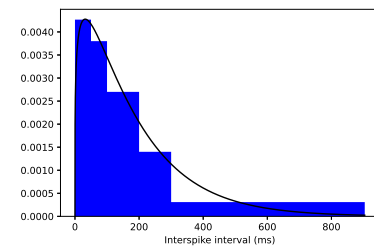


Fig. 4. Resulting ISI histogram and adjusted gamma for parameters:  $\mu = 0$ ,  $\sigma = 1.7$ .

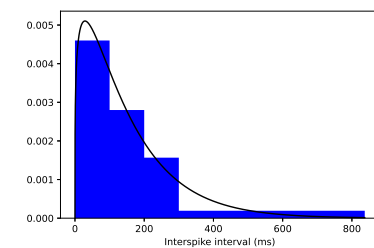


Fig. 5. Resulting ISI histogram and adjusted gamma for parameters:  $\mu = 0.2$ ,  $\sigma = 1.7$ .

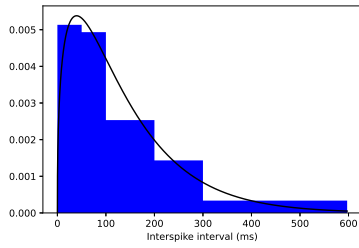


Fig. 6. Resulting ISI histogram and adjusted gamma for parameters:  $\mu = 0.4$ ,  $\sigma = 1.7$ .

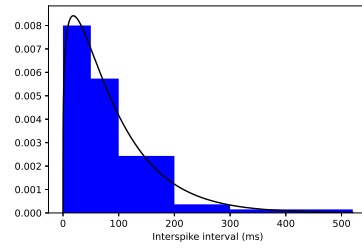


Fig. 9. Resulting ISI histogram and adjusted gamma for parameters:  $\mu = 0.4$ ,  $\sigma = 1.9$ .

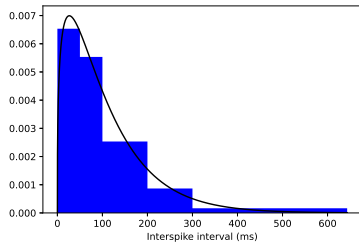


Fig. 7. Resulting ISI histogram and adjusted gamma for parameters:  $\mu = 0$ ,  $\sigma = 1.9$ .

TABLE II

ESTIMATED GAMMA PARAMETERS AND  $p$ -VALUE FOR CHI-SQUARE GOODNESS OF FIT TEST ( $\mu$  AND  $\sigma$  IN  $\mu A/CM^2$ ).

$(\mu, \sigma)$	$\hat{\eta}$	$\hat{\lambda}$	$p$ -value	Entropy (nats)
(0, 1.5)	1.169	0.003	0.91	6.93
(0, 1.7)	1.215	0.007	0.87	6.18
(0, 1.9)	1.332	0.013	0.58	5.64
(0.2, 1.5)	0.983	0.003	0.052	6.77
(0.2, 1.7)	1.240	0.008	0.61	5.99
(0.2, 1.9)	1.406	0.015	0.70	5.54
(0.4, 1.5)	1.192	0.004	0.07	6.63
(0.4, 1.7)	1.410	0.010	0.33	5.88
(0.4, 1.9)	1.259	0.014	0.13	5.48

Table II also presents the computed information measures. The differential entropy of a gamma distribution  $f$  with parameters  $\eta$  and  $\lambda$  is given as [26]:

$$h(f) = (1 - \eta_f)\psi(\eta_f) - \ln \lambda_f + \ln \Gamma(\eta_f) + \eta_f, \quad (11)$$

where  $\psi(x)$  is the digamma function defined by  $\psi(x) =$

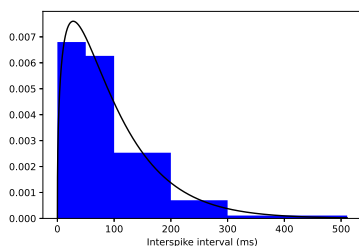


Fig. 8. Resulting ISI histogram and adjusted gamma for parameters:  $\mu = 0.2$ ,  $\sigma = 1.9$ .

$\Gamma'(x)/\Gamma(x)$ . If we apply this formula with the different estimated values for  $\eta$  and  $\lambda$ , we obtain the entropies shown in Table II, last column, in nats.

Observing the entropy values in the last column of Table II, we notice some interesting characteristics. Firstly, keeping the mean value constant, we see that as the variance of the input current increases, the entropy of ISIs diminishes (at least for the tested values of synaptic input), which is a quite counterintuitive fact. This fact is possibly due to the neuronal dynamics. A greater diffusion parameter may cause the neuron to spike more often, reaching its refractory period. Secondly, we may calculate the deviation in entropies and compare to which parameter, drift or diffusion, it is more sensible to. For example, fixing the diffusion parameter  $\sigma = 1.5$  of the applied synaptic current, we obtain:

$$\begin{aligned} |\Delta h| &= |h(f_{0,1.5}) - h(f_{0.2,1.5})| \approx 0.1 \text{ nats}, \\ |\Delta h| &= |h(f_{0.2,1.5}) - h(f_{0.4,1.5})| \approx 0.2 \text{ nats}, \\ |\Delta h| &= |h(f_{0,1.5}) - h(f_{0.4,1.5})| \approx 0.3 \text{ nats}. \end{aligned}$$

(12)

Also, when fixing the values for  $\sigma = 1.7$  and  $\sigma = 1.9$ , we obtain:

$$\begin{aligned} |\Delta h| &= |h(f_{0,1.7}) - h(f_{0.2,1.7})| \approx 0.2 \text{ nats}, \\ |\Delta h| &= |h(f_{0.2,1.7}) - h(f_{0.4,1.7})| \approx 0.1 \text{ nats}, \\ |\Delta h| &= |h(f_{0.4,1.7}) - h(f_{0,1.7})| \approx 0.3 \text{ nats}, \\ |\Delta h| &= |h(f_{0,1.9}) - h(f_{0.2,1.9})| \approx 0.1 \text{ nats}, \\ |\Delta h| &= |h(f_{0.2,1.9}) - h(f_{0.4,1.9})| \approx 0.0 \text{ nats}, \\ |\Delta h| &= |h(f_{0.4,1.9}) - h(f_{0,1.9})| \approx 0.1 \text{ nats}. \end{aligned}$$

Thus, fixing the diffusion parameter, and deviations of  $\Delta\mu = 0.2$  or  $0.4$ , the greatest found value for entropy deviation was approximately 0.3 nats.

On the other hand, fixing the drift parameter, we obtain:

$$\begin{aligned}
 |\Delta h| &= |h(f_{0,1.5}) - h(f_{0,1.7})| \approx 0.7 \text{ nats,} \\
 |\Delta h| &= |h(f_{0,1.7}) - h(f_{0,1.9})| \approx 0.6 \text{ nats,} \\
 |\Delta h| &= |h(f_{0,1.9}) - h(f_{0,1.5})| \approx 1.3 \text{ nats,} \\
 |\Delta h| &= |h(f_{0,2,1.5}) - h(f_{0,2,1.7})| \approx 0.8 \text{ nats,} \\
 |\Delta h| &= |h(f_{0,2,1.7}) - h(f_{0,2,1.9})| \approx 0.5 \text{ nats,} \\
 |\Delta h| &= |h(f_{0,2,1.9}) - h(f_{0,2,1.5})| \approx 1.3 \text{ nats,} \\
 |\Delta h| &= |h(f_{0,4,1.5}) - h(f_{0,4,1.7})| \approx 0.7 \text{ nats,} \\
 |\Delta h| &= |h(f_{0,4,1.7}) - h(f_{0,4,1.9})| \approx 0.4 \text{ nats,} \\
 |\Delta h| &= |h(f_{0,4,1.9}) - h(f_{0,4,1.5})| \approx 1.1 \text{ nats,}
 \end{aligned}$$

Observing these calculations, we see that ISI distribution is extremely sensible to the magnitude of  $\sigma$ , the noise of the applied current, when compared to similar changes in magnitude of drift parameter. When deviation in the synaptic parameters are of  $\Delta\mu = \Delta\sigma = 0.2$ , the changes in entropy are of the order of twice to eight times greater when varying extrinsic noise than when varying mean value of synaptic current. When deviation in the synaptic parameters are of  $\Delta\mu = \Delta\sigma = 0.4$ , differences in entropy are about four to ten times greater when considering noise than when considering mean synaptic input. Since entropy is a measure of uncertainty of a random variable, from these results we observe that neuronal temporal coding is deeply related to the noise of the environment that neuron is submitted to.

Interestingly, there is a similar result reported by [24] in the context of rate coding, which showed that when white noise current is applied in Hodgkin-Huxley neuron, the firing rate of the neuron is more sensible to the variance of the applied current than to its mean value, providing us one more evidence about noise contribution to neuronal activity and information processing.

#### IV. CONCLUSION

In this paper we simulated Hodgkin-Huxley model in response to different white noise synaptic currents with certain mean and standard deviation. We observed that, for the tested values of synaptic input and keeping the mean value constant, the differential entropy of ISIs distributions diminishes as the standard deviation of the input increases. Also, our results show that, in a scenario such as the cortex of animals, where synaptic input may be modelled as white noise and ISI may be modelled as gamma distributed, information measures of ISIs are very sensible to changes in the diffusion parameter, which is related to the noise the neuron is submitted to. Specifically, differential entropy of ISIs changes dramatically with changes in the standard deviation magnitude in comparison to similar changes in the mean value of the pattern. Since in temporal coding information is encoded through ISI, we concluded that neurons are very sensible to extrinsic noise in this mechanism of information processing.

#### REFERENCES

- [1] Riccardo Barbieri, Michael C Quirk, Loren M Frank, Matthew A Wilson, and Emery N Brown. Construction and analysis of non-poisson stimulus-response models of neural spiking activity. *Journal of neuroscience methods*, 105(1):25–37, 2001.
- [2] Mark Bear, Barry Connors, and Michael A Paradiso. *Neuroscience: Exploring the brain*. Lippincott Williams & Wilkins, 2007.
- [3] Roberto Benzi, Alfonso Sutera, and Angelo Vulpiani. The mechanism of stochastic resonance. *Journal of Physics A: mathematical and general*, 14(11):L453, 1981.
- [4] Christopher M Bishop and Nasser M Nasrabadi. *Pattern recognition and machine learning*, volume 4. Springer, 2006.
- [5] Thomas M. Cover and Joy A. Thomas. *Elements of Information Theory*. Wiley-Interscience, 2006.
- [6] Wainrib Gilles, Thieullen Michele, and Pakdaman Khashayar. Intrinsic variability of latency to first-spike. *Biological cybernetics*, 103(1):43–56, 2010.
- [7] Daqing Guo, Matjaž Perc, Tiejun Liu, and Dezhong Yao. Functional importance of noise in neuronal information processing. *EPL (Europhysics Letters)*, 124(5):50001, 2018.
- [8] Alan L Hodgkin and Andrew F Huxley. A quantitative description of membrane current and its application to conduction and excitation in nerve. *The Journal of physiology*, 117(4):500, 1952.
- [9] Shiro Ikeda and Jonathan H Manton. Spiking neuron channel. In *2009 IEEE International Symposium on Information Theory*, pages 1589–1593. IEEE, 2009.
- [10] Eugene M Izhikevich. *Dynamical systems in neuroscience*. MIT press, 2007.
- [11] Abram Meerovich Kagan, Yu V Linnik, and Calyampudi Radhakrishna Rao. *Characterization problems in mathematical statistics*. Wiley-Interscience, 1973.
- [12] Eric R Kandel, James H Schwartz, Thomas M Jessell, Steven Siegelbaum, A James Hudspeth, and Sarah Mack. *Principles of neural science*, volume 4. McGraw-hill New York, 2000.
- [13] Harold J. Larson. *Introduction to Probability Theory and Statistical Inference*. John Wiley and Sons, 1982.
- [14] Marie Levakova, Massimiliano Tamborino, Lubomir Kostal, and Petr Lansky. Presynaptic spontaneous activity enhances the accuracy of latency coding. *Neural Computation*, 28(10):2162–2180, 2016.
- [15] Meng Li and Joe Z Tsien. Neural code — neural self-information theory on how cell-assembly code rises from spike time and neuronal variability. *Frontiers in cellular neuroscience*, 11:236, 2017.
- [16] Zachary F Mainen and Terrence J Sejnowski. Reliability of spike timing in neocortical neurons. *Science*, 268(5216):1503–1506, 1995.
- [17] Brenton Maisel and Katja Lindenberg. Channel noise effects on first spike latency of a stochastic hodgkin-huxley neuron. *Physical Review E*, 95(2):022414, 2017.
- [18] Athanasios Papoulis and S. Unnikrishna Pillai. *Probability, Random Variables and Stochastic Processes*. Mc Graw Hill, 2002.
- [19] Arkady S. Pikovsky and Jürgen Kurths. Coherence resonance in a noise-driven excitable system. *Phys. Rev. Lett.*, 78:775–778, Feb 1997.
- [20] Alexander N Pisarchik, Vladimir A Maksimenko, Andrey V Andreev, Nikita S Frolov, Vladimir V Makarov, Maxim O Zhuravlev, Anatasija E Runnova, and Alexander E Hramov. Coherent resonance in the distributed cortical network during sensory information processing. *Scientific Reports*, 9(1):1–9, 2019.
- [21] Alex Roxin, Nicolas Brunel, David Hansel, Gianluigi Mongillo, and Carl van Vreeswijk. On the distribution of firing rates in networks of cortical neurons. *Journal of Neuroscience*, 31(45):16217–16226, 2011.
- [22] Shigeru Shinomoto, Keisetsu Shima, and Jun Tanji. Differences in spiking patterns among cortical neurons. *Neural computation*, 15(12):2823–2842, 2003.
- [23] Sangmin Song, Ji Ah Lee, Ilya Kiselev, Varun Iyengar, Josef G Trapani, and Nesity Tania. Mathematical modeling and analyses of interspike-intervals of spontaneous activity in afferent neurons of the zebrafish lateral line. *Scientific reports*, 8(1):1–14, 2018.
- [24] PHE Tiesinga, Jorge V José, and Terrence J Sejnowski. Comparison of current-driven and conductance-driven neocortical model neurons with hodgkin-huxley voltage-gated channels. *Physical review E*, 62(6):8413, 2000.
- [25] Henry C Tuckwell. Spike trains in a stochastic hodgkin-huxley system. *BioSystems*, 80(1):25–36, 2005.
- [26] Yaming Yu. Complete monotonicity of the entropy in the central limit theorem for gamma and inverse gaussian distributions. *Statistics & Probability Letters*, 79(2):270–274, 2009.
- [27] Trevor M Zohar, Oran Shackleton, Israel Nelken, Alan R Palmer, and Maoz Shamir. First spike latency code for interaural phase difference discrimination in the guinea pig inferior colliculus. *Journal of Neuroscience*, 31(25):9192–9204, 2011.